ANALELE UNIVERSITATII BUCUREŞTI

Department of Physical Chemistry
4-12 Regina Elisabeta Blvd, District 3, Bucharest
phone: +40-21-3143508; fax: +40-21-3159249
*p*ISSN: 1220-871X *e*ISSN: 1844-0401

ARS DOCENDI PUBLISHING HOUSE
Sos. Panduri 90, District 5 Bucharest
phone/fax: +40-21-4102575
e-mail: arsdocendi@yahoo.com

CHARACTERIZATION BY DYNAMIC THERMAL METHODS OF SOME BIS-AZOPOLYETHERS WITH AN OCTAMETHYLENE SPACER

N. Hurduc *, Gabriela Lisa, Silvia Alazaroaie and Natalia Hurduc **

abstract: This paper presents the characterization by dynamic thermal methods of some bis-azopolyethers with an octamethylene spacer. For the thermal analysis we used a MOM-Budapest derivatograph which enables the simultaneous recording of the thermogravimetric (TG), derivative thermogravimetric (DTG) and differential thermal (DTA) analyses. The recordings were performed in the air – static conditions, at different heating rates (10, 15, 20 °C/min), whereas the other working parameters remained constant, in order to obtain comparable data. The performed study led to some conclusions on structure – thermostability – degradation mechanism. The kinetic characteristics, correlated with the thermogravimetric ones, illustrate the degradation via successive reactions and the complexity of the second degradation stage, due to the static division of the methylene groups depending on structure and heating rate.

key words: azopolyethers; thermal degradation; kinetic characteristics; degradation mechanism.

received: February 01, 2011 *accepted*: April 11, 2011

1. Introduction

The compounds whose thermal stability is analyzed in this paper are part of a class of special matter, liquid crystal polymers, with mesophases specific to small-molecule liquid crystals, preserving, at the same time, many of the useful properties of polymers.

The thermal stability of the synthesized materials is one of the most important requirements for the discovery of new properties [1-4]. Since thermotropic liquid crystals are materials where the arrangement capacity in liquid crystal structures occurs within a specific temperature range and involves the increase of the system temperature, it is easy to understand the major role that thermal stability plays for these compounds.

The study of the thermal behavior of polymers establishes the structure-thermostability-degradation mechanism dependence necessary for getting to know the application field, the processing conditions and the valorization of industrial waste.

* Gheorghe Asachi Technical University, Chemical Engineering and Environment Protection Faculty, B-dul D. Mangeron, no. 71, 700050 - Iasi, Romania *corresponding author e-mail*: gapreot@ch.tuiasi.ro
** Al. I. Cuza University Iasi, Faculty of Chemistry, B-dul Carol I, no. 11, 700506 – Iasi, Romania

For this purpose we carried on our studies concerning the behavior of some polyethers with a flexible spacer of a methylene[5-12] type, with bisazocopolyethers with octamethylene spacer.

2. Experimental

Synthesis and samples preparation

The analyzed copolyethers were synthesized via the interphase transfer catalysis method in a liquid/liquid system [13,14], using bisphenols 4,4'-bis(4 hydroxy-azobenzene)diphenyl and 4,4' hydroxydiphenyl, in different feeding ratios, and 1,8 dichlorooctane as spacer.

Schematically, the synthesis reaction can be rendered as follows:

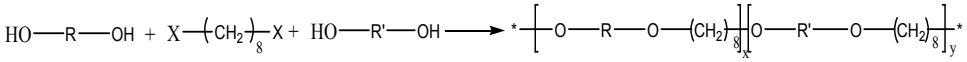

were:

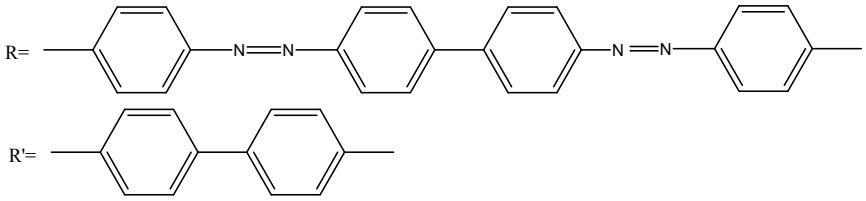

x/y = 3/1	x/y = 1/1	x/y = 1/3
sample 1	sample 2	sample 3

Reaction conditions: 85°C temperature, tetramethylammonium bromide as catalyst, NaOH 40% concentration, organic solvent – nitrobenzene, and reaction time – 5 hours. The copolymerization ratios and the numerical molecular weights (Mn) were calculated by using the end chain signals ^{1}H-NMR spectra which were recorded on a BRUKER AVENCE 300 MHz device with DMSO-d_6 as a solvent. Differential scanning calorimetry (DSC) thermograms were recorded on a METTLER 12E device with a heating/cooling rate of 10°C min^{-1}. Optical microscopy studies in polarized light were performed on an OLYMPUS BH-2 device equipped with a LINKAM TP 92 temperature controller. Some characteristics of the synthesized polymers are presented in Table 1.

According to the theoretical conformational analyses, 4,4'-bis(4 hydroxy-azobenzene)diphenyl presents two minimum energy conformations [15].

The energy differences between the two conformers are small, the isomer corresponding to structure 2 (the minimum energy is smaller by 6% than that for structure 1) being slightly favored (Figs. 1 and 2). This suggests the possibility of chain occurrence of both conformations, without a vital impact from a geometric perspective, since the asymmetry coefficients have close values (4.4 for structure 1 and 3.7 for structure 2).

Table 1 Some characteristics of the synthesized copolyethers.

Sample code	Copolymer composition	Molecular mass Mn	Phase transitions
sample 1	2.7/1	3200	K → 215 °C (LCe)
sample 2	1/1.1	3500	K → 220 °C (LCe)
sample 3	1/2.9	2800	K → 200 °C (LCe)

K-crystalline phase; LCe – liquid crystalline phase (enantiotropic behaviour)

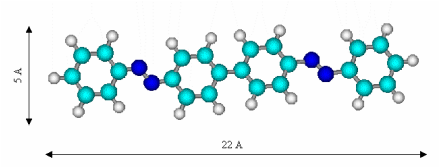

Fig. 1 *Minimum energy conformations for sample 1.*

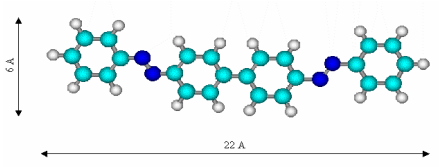

Fig. 2 *Minimum energy conformations for sample 2.*

Thermal behavior of copolyethers

The study of the thermal behavior of copolyethers was performed with the help of the MOM-Budapest derivatograph which enables the simultaneous recording of the thermogravimetric, derivative thermogravimetric and differential thermal analyses. The recordings were performed in the air – static conditions, at different heating rates (10, 15, 20 °C/min). The other working parameters remained constant for the purposes of obtaining comparable data.

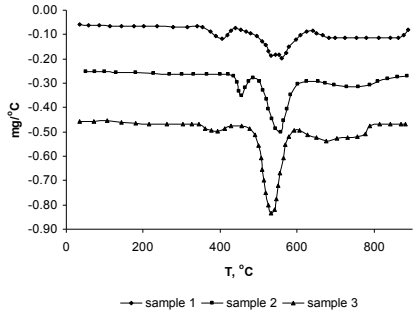

Fig. 3 *DTG curves at the same heating rate of 10 °C/min.*

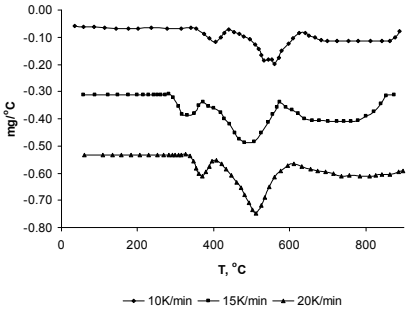

Fig. 4 *DTG curves for sample 1 at different heating rates.*

3. Results and discussion

Fig. 3 presents the DTG curves for the samples analyzed at the same heating rate of 10°C/min. We noticed the existence of three degradation stages, regardless of the molar ratio of the comonomers. Fig. 4 presents the DTG curves for sample 1, in order to highlight the influence of the heating rate. We may notice the preservation of the three degradation stages, regardless of the heating rate. The thermogravimetric characteristics for various

heating rates are registered in Table 2. The analysis of the initial degradation temperatures is indicative of the influence of the heating rate and structure. The best thermostability corresponds to the 1/1 molar ratio. The high polarity of the mesogens and the parallel arrangement of the spacer, due to the even/odd effect imposed by the number of methylene groups, probably lead to the orderly packaging of the macromolecular chains, accounting for the high thermostability of sample 2. The temperature ranges and the mass losses corresponding to the degradation stages are not considerably influenced by the heating rate. The higher differences appear depending on the structure. The existence of the three stages is indicative of the degradation via successive reactions. In order to obtain additional information about the fragmentation of the sequences, we made a calculation that we compared to the thermogravimetric analysis data (Table 3). By correlating the computed data with the thermogravimetric ones, the following scheme can be accepted:

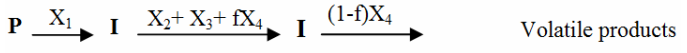

Table 2 Thermogravimetric data at different heating rates.

Sample	dT/dt (K/min)	ΔT_1 (°C)	W_1 %	ΔT_2 (°C)	W_2 %	ΔT_3 (°C)	W_3 %
	10	300-405	11.11	405-620	42.85	620-880	46.03
1	15	270-410	11.54	410-600	46.15	600-820	42.20
	20	280-430	15.38	430-660	41.53	660-940	43.07
	10	380-450	9.43	450-610	50.94	600-900	39.62
2	15	370-460	9.80	450-600	52.94	600-900	37.25
	20	340-490	10.41	490-640	56.25	640-880	33.33
	10	300-400	6.25	400-545	59.32	545-760	34.43
3	15	260-430	9.83	430-620	70.49	620-760	19.57
	20	310-460	6.25	460-615	65.07	615-840	28.57

dT/dt – heating rates; ΔT – temperature range in each degradation stages; W – the weight loss corresponding to the degradation stage

Table 3 Mass losses calculated in comparison with the ATG data.

Sample	dT/dt (K/min)	ATG data			Mass losses calculated				f
		W_1 %	W_2 %	W_3 %	X_1 (N_2) %	X_2 $(-CH_2-)_8$ %	X_3 (O_2) %	X_4 (Ar) %	
	10	11.11	42.85	46.03					1/4
1	15	11.54	46.15	42.20	9.29	24.78	7.07	58.84	1/4
	20	15.38	41.53	43.07					1/4
	10	9.43	50.94	39.62					1/4
2	15	9.80	52.94	37.25	7.00	28.00	8.00	57.00	1/4
	20	10.41	56.25	33.33					1/3
	10	6.25	59.32	34.43					1/3
3	15	9.83	70.49	19.57	4.02	32.18	9.18	54.59	2/3
	20	6.25	65.07	28.57					1/2

According to the present data, the nitrogen is lost during the first stage, since the nitro groups are the most unstable ones. During the second stage, the spacer and some of the aromatic cycles split off. The remaining aromatic groups degrade via thermal oxidation. The succession of the relations is also suggested by the analysis of the DTA curves in Fig. 5, respectively the succession of some exo and endo thermal effects.

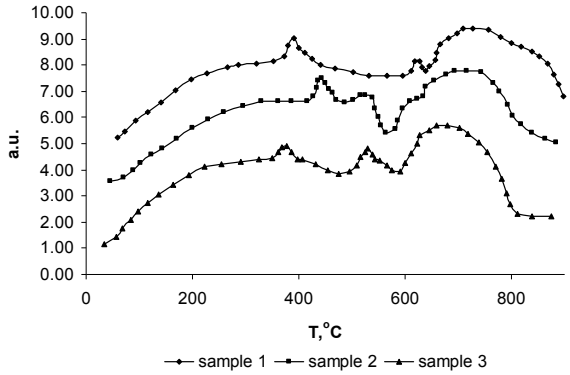

Fig. 5 *DTA curves at the same heating rate of 10 °C/min.*

The first and the last stage are accompanied by exothermal effects, whereas the second stage is accompanied by an endothermal process. The symmetry of the first peak illustrates a unitary process, whereas the last peak is specific to thermal oxidation.

$$\ln\frac{F(\alpha)}{T^2} = \ln\left[\frac{A}{a}\cdot\frac{R}{Ea}\cdot\left(1-\frac{2RT}{E}\right)\right] - \frac{E}{R}\cdot\frac{1}{T} \qquad (1)$$

where T is the temperature, $\propto$ - the degree of conversion, "a" – the heating rate, A – pre-exponential factor, R – the universal gas constant, $F(\propto)$ – the conversion function and E – the apparent activation energy.

Table 4 Kinetic characteristics assessed via the method Coats-Redfern at different heating rates.

Sample	dT/dt (K/min)	Stage I		Stage II		Stage III	
		n	E(kJ/mol)	n	E(kJ/mol)	n	E(kJ/mol)
1	10	0	62.09	1	146.26	0	49.32
	15	0	32.82	1	203.42	0	57.44
	20	0	50.02	1	138.05	0	63.82
2	10	0	95.78	1	225.96	0	58.02
	15	0	38.29	1	143.60	0	68.92
	20	–	–	1	230.48	0	104.06
3	10	0	58.02	1	287.20	0	31.37
	15	0	38.29	1	168.18	0	46.30
	20	–	–	1	239.33	0	120.45

n – reaction order, E – apparent activation energy

It is graphically represented as $\ln(F(\alpha)/T^2)$ depending on $1/T$ for various values of the conversion function corresponding to the reaction order and, if the dependence is linear, the form of the function indicates the reaction order, and the apparent activation energy is calculated from the slope of the straight line. The obtained values are presented in Table 4.

The apparent activation energies confirm the mechanism proposed via successive reactions. The first stage occurs with smaller energy consumption, since the nitro groups are the most sensitive to thermal attack. The fragmentation of the spacer, as well as of some aromatic cycles, during the second stage, involves the splitting up of the C-C bonds, with large energy consumption in comparison with the last stage, which is accompanied by a strong exothermal effect. The reaction orders for the first and the last stage illustrate the importance of the transportation – diffusion phenomena. The heating rate influences the apparent activation energy, confirming the complexity of the degradation mechanism, especially during the second degradation stage.

In conditions of maximum degrading rate we applied the Kissinger method [17] which for estimating the activation energy uses the following computational equation:

$$\ln\frac{a}{T_M^2} = \ln\frac{AR}{Ea} - \frac{Ea}{R}\cdot\frac{1}{T_M} \tag{2}$$

where a is the heating rate (10°C/min 15°C/min and 20°C/min) and T_M – the temperature at the maximum rate of weight loss. The resulting kinetic parameters of this method are shown in Table 5. Depending on the chemical structure of the copolyethers, the apparent activation energies have different values and confirming the complexity of the degradation mechanism.

Table 5 Kinetic characteristics assessed via the method Kissinger.

Sample	Stage I		Stage II		Stage III	
	n	E(kJ/mol)	n	E(kJ/mol)	n	E(kJ/mol)
1	1	88.86	1	127.08	1	106.17
2	–	–	–	–	1	139.08
3	1	61.58	1	111.79	1	76.71

n – reaction order, E – apparent activation energy

The application of the Freman – Carroll [18] method for the kinetic processing of the thermogravimetric data makes use of the equation below:

$$\frac{\Delta\ln(\mathrm{d}\alpha/\mathrm{d}t)}{\Delta\ln(1-\alpha)} = n - \frac{Ea}{R}\cdot\frac{\Delta(1/T)}{\Delta\ln(1-\alpha)} \tag{3}$$

The graphical representation of the $\frac{\Delta\ln(\mathrm{d}\alpha/\mathrm{d}t)}{\Delta\ln(1-\alpha)}$ ratio depending on $\frac{\Delta(1/T)}{\Delta\ln(1-\alpha)}$ leads to a straight line whose intercept with the ordinate represents the reaction order and the apparent activation energy is calculated from the slope. The computed values are presented in Table 6. The apparent activation energy and the influence of the heating rate confirm the complexity of the degradation in the second stage, which can be attributed to the big number of methylene groups in the spacer, which split off into fragments with a variable

number of carbon atoms depending on the heating rate, similarly to polyethylene [19]. The table also includes the critical temperature, calculated with the help of the equation proposed by Gorbakev [20]:

$$\frac{1}{T_{cr}} = \frac{1}{T_M} + \frac{R}{E}\ln\frac{E \cdot a}{RT_M^2} \quad (4)$$

where T_M represents the temperature corresponding to the maximum degradation rate, E – the apparent activation energy, "a" – the heating rate, R – the universal gas constant and T_{cr} – the critical or isokinetic temperature. The value of the critical temperature is close to the one corresponding to the maximum degradation rate.

Table 6 Kinetic characteristics assessed via the method Freeman-Carroll.

Sample	dT/dt (K/min)	n	E(kJ/mol)	lnA	Sp	TM (K)	Tcr (K)
	10	1	191.47	28.21	6.78	795	856
1	15	1	213.56	31.87	6.70	793	785
	20	0.4	130.65	20.79	6.20	853	870
	10	2	239.33	32.78	7.30	803	755
2	15	1.5	341.45	30.90	6.70	793	794
	20	1	280.69	42.46	6.59	818	819
	10	1	297.70	46.80	6.34	773	777
3	15	1	230.34	35.56	6.54	803	804
	20	2	326.62	45.18	7.22	813	824

n – reaction order; E – apparent activation energy; A – preexponential factor, Sp= E/ln$A$ – compensation parameter, T_M – temperature corresponding to the highest degradation speed , T_{cr} – critical temperature.

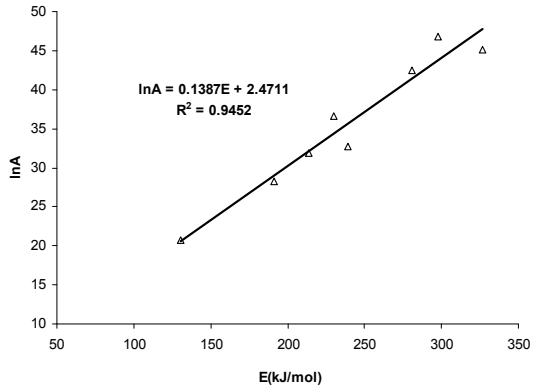

Fig. 6 *The pre-exponential factor dependence as function of the activation energy.*

The compensation parameter (Sp) suggests a similar degradation mechanism. In order to make sure, we verified the validity of the compensation equation (Fig. 6), ln A = aE + b, where A is the pre-exponential factor, E – the apparent activation energy, a and b are the compensation coefficients. For this purpose, we graphically monitored ln$A$ = f(E). Linear

dependence confirms a similar degradation mechanism – respectively successive reactions. The parameters of the straight line lead to the following compensation equation: lnA = 0.1387E – 2.4711. The complexity of the degradation mechanism is also confirmed by the Flynn-Wall chart (Fig. 7) [21]. The existence of the inflexion points is indicative of modifications in the nature of the micromolecules eliminated at various heating rate [19].

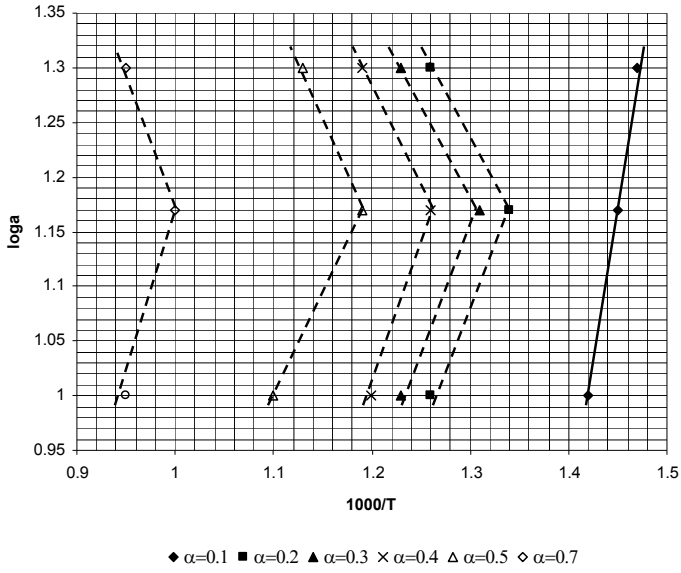

Fig. 7 *Flynn-Wall chart for the samples.*

4. Conclusions

The performed study leads to a series of conclusion concerning thermostability and degradation mechanisms. Copolyethers have a thermostability which ranges between 260-380°C, depending on their structure and heating rate. Sample 2 – 1/1 molar ratios has the best thermostability. The kinetic characteristics, correlated with the thermogravimetric ones, illustrate the degradation via successive reactions and the complexity of the second degradation stage, due to the statistic division of the methylene groups depending on their structure and heating rate.

Acknowledgements. The authors would like to thank to the ANCS for the financial support (Project CEA C101). The thermal stability studies were effectuated on the Interdisciplinary Research Platform for Multifunctional, High Performance Polymers and financial supported by by CNCSIS –UEFISCSU, project number 64, PNII – IDEI 600/2007.

REFERENCES

1. Chuan-hua, G., Meng-yi, C., Jia-ni, N., Ji-jun, H., Xiao-ming, X., Wei-wei, L., Qiang, Z. (2010) *Chinese J. Polym. Sci.* **28**, 219.

2. Vyazovkin, S., Dranca, I., Fan, X., Advincula, R. (2004) *Macromol. Rapid Commun.* **25**, 498.
3. Xiao-jun, W., Mei-lin, Z., Jing, L., Gang, Z., Jie, Y. (2010) *Chinese J. Polym. Sci.* **28**, 85.
4. Devamani, S., Sundaram, M., Sivashankaran, N., Subramanan, B., Sengodan, S. (2009) *Chinese J. Polym. Sci.* **27**, 761.
5. Tarus, A., Hurduc, N., Catanescu, O., Cobzaru, C., Hurduc, N. (2000) *Polym. Degrad. Stabil*. **68**, 87.
6. Hurduc, N., Prajinaru, M., Donose, B., Pavel, D., Hurduc, N. (2001) *Polym. Degrad. Stabil.* **72**, 441.
7. Creanga, A., Hurduc, N., Pokol, G., Novák, C., Alazaroaie, S., Hurduc, N. (2003) *J. Therm. Anal. Cal*. **70,** 877.
8. Sfichi-Damian, C., Hurduc, N., Hurduc, N., Shanks, R., Yarovski, I., Pavel D. (2003) *Comput. Mat. Sci.* **27**, 393.
9. Prajinaru, M., Hurduc, N., Alazaroaie, S., Catanescu, O., Hurduc, N. (2006) *Cent. Eur. J. Chem*. **4,** 387.
10. Creanga, A., Pokol, G., Hurduc, N., Novák, C., Alazaroaie, S., Hurduc, N. (2004) *J. Therm. Anal. Cal.* **66**, 859.
11. Hurduc, N., Damian, C., Tarus, A., Toader, V., Hurduc, N. (2005) *Cent. Eur. J. Chem.* **3**, 53.
12. Lisa, G., Hurduc, N., Alăzăroaie, S., Hurduc, N. (2008) *Polym. Bull.* **61**, 759.
13. Alazaroaie, S., Hurduc, N., Scutaru, D., Dumitrascu, A., Petraru, L., Simionescu, C.I. (2003) *J. Macromol. Sci.- Pure and Appl. Chemistry.* **40**, 1241.
14. Hurduc, N., Damian, C., Lisa, G., Toader, V. (2007) *High Perform. Polym*. **19**, 477.
15. Pavel, D., Shanks, R., Sangari, S., Alazaroaie, S., Hurduc, N. (2004) *Mater. Plast.* **41**, 41.
16. Coats, A.W., Redfern, J.P. (1964) *Nature* **201**, 68.
17. Kissinger, H E. (1957) *Anal. Chem.* **29**, 1702.
18. Freeman, E. S., Carroll, B. (1958) *J. Phys. Chem*. **62,** 394.
19. Schneider, I. A., Hurduc N. (1977) *Makromol. Chem.***178**, 547.
20. Gorbachev, V.M. (1975) *J. Thermal Anal.* **6**, 349.
21. Flynn, J. H., Wall, L. A., Quick, A. (1966) *Polymer Letters* **4**, 323.